Emission Abatement Technology

at the Technical University Ostrava

Project AKTION 58p21

July 2011

edited by

Matthias Kuba[a]

tutored by

Lenka Kuboňová[b], Marcel Šihor[b], Ivana Troppová[b]

supervised by

Prof. Kamila Koci[b], Prof. Lucie Obalová[b], Prof. Franz Winter[a]

[a] *Vienna University of Technology, Getreidemarkt 9/166, 1060 Vienna, Austria*

[b] *Technical University Ostrava, 17.listopadu 15, 708 33 Ostrava, Czech Republic*

Table of Contents

Photocatalytic Reduction of CO_2

Introduction

The global concentration of greenhouse gases in our atmosphere is increasing dramatically. The main contributor to the greenhouse effect is carbon dioxide (CO_2) therefore the reduction of CO_2 has become one of the most important research topics. Since CO_2 is a stable compound, the reduction of CO_2 is difficult. The conversion by force only can be realized under severe conditions, high pressure and high temperature would be necessary. The idea behind using photocatalysts to reduce CO_2 is that the greenhouse gas can be transformed into more advantageous compounds. The products are valuable chemicals, such as methanol, ethanol and methane. [1]

Experiments

In all experiments the used catalyst was titanium dioxide (TiO_2). The most important advantages of titania photocatalysts are their strong chemical resistance and their low operational temperature. The efficiency of the photocatalytic reduction is relatively low and an increase of yield is necessary. Since TiO_2 can only be excited by high energy UV irradiation with a wavelength shorter than 387,5nm, efforts have been made to improve the photocatalytic activity of TiO_2. One way to gain improvement for example is doping the TiO_2 with silver so that the light absorption range of TiO_2 is extended. The Ag content positively influences the yields of CO_2 photocatalytic reduction. [2]

The reduction of carbon dioxide using photocatalysts was carried out in a batch reactor with a length of 35 cm and a width of 3.5 cm. The internal volume was 380 cm^3. The suspended catalyst inside the reactor was illuminated by an 8 W Hg lamp. The block scheme of the apparatus is shown in Fig. 1. The CO_2 was irradiated with UV light at room temperature and atmospheric pressure.
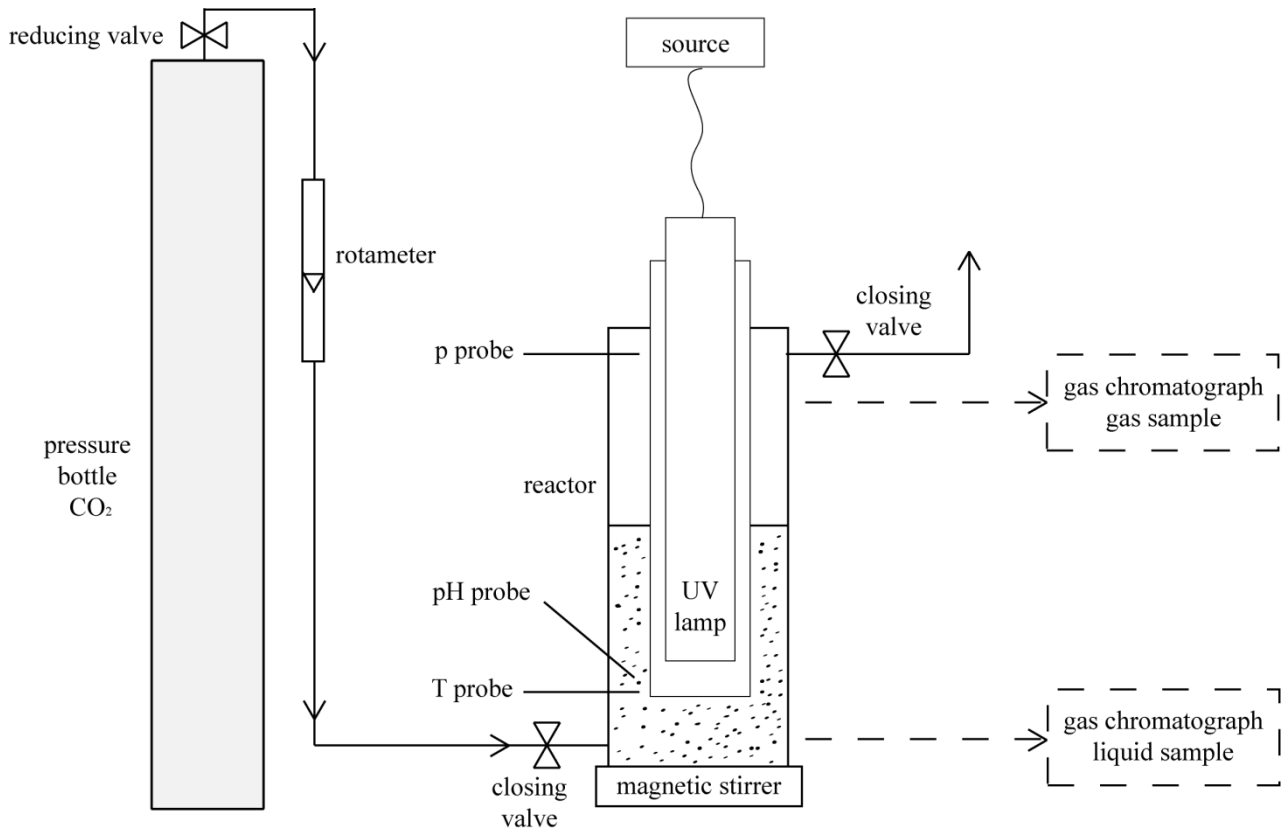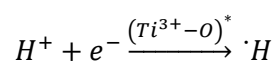
Fig. 1: Block scheme of the apparatus for photocatalytic reduction of carbon dioxide

Chemical reaction

The initiation of the reaction is caused by the UV-light. The following reactions show the secession of an electron and the formation of H^+ and the H radical.

$$TiO_2 \xrightarrow{hv} e^-(TiO_2) + h^+(TiO_2)$$

$$e^-(TiO_2) + h^+(TiO_2) \xrightarrow{hv} \Delta$$

$$4h^+ + 2H_2O \xrightarrow{(Ti^{3+}-O)^*} O_2 + 4H^+$$

$$H^+ + e^- \xrightarrow{(Ti^{3+}-O)^*} {}^\cdot H$$
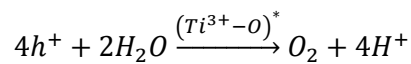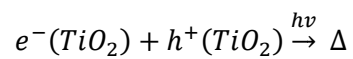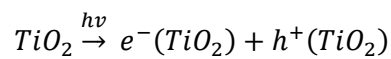
As it can be seen in the following propagation steps the CO_2 is then transformed into CO and OH^- and further the CO is turned into C and OH^-. The OH^- forms an OH radical.

$$CO_2 + e^- \xrightarrow{(Ti^{3+}-O)^*} O - \cdot C - O^-$$

$$O - \cdot C - O^- + \ \cdot H \xrightarrow{(Ti^{3+}-O)^*} CO + OH^-$$

$$CO + e^- \xrightarrow{(Ti^{3+}-O)^*} \cdot CO^-$$

$$\cdot CO^- + \ \cdot H \xrightarrow{(Ti^{3+}-O)^*} C + OH^-$$

$$OH^- + h^+ \xrightarrow{(Ti^{3+}-O)^*} \cdot OH$$
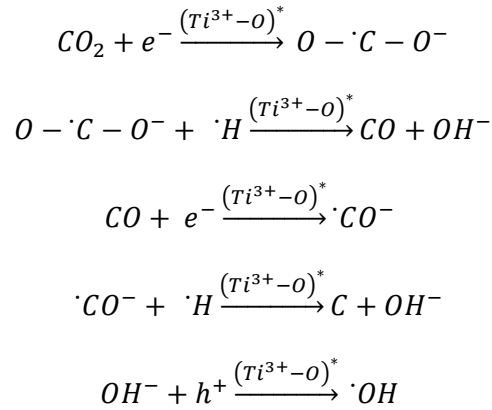
The methane radical is formed in four separate propagation steps, in each step the carbon reacts with an H radical.
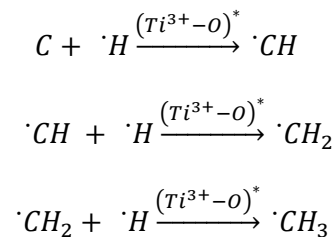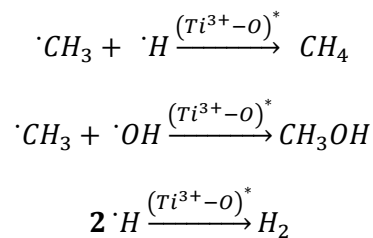
$$C + \ \cdot H \xrightarrow{(Ti^{3+}-O)^*} \cdot CH$$

$$\cdot CH + \ \cdot H \xrightarrow{(Ti^{3+}-O)^*} \cdot CH_2$$

$$\cdot CH_2 + \ \cdot H \xrightarrow{(Ti^{3+}-O)^*} \cdot CH_3$$

There are three possibilities of termination, in which the radicals recombine with another radical species. The first is the formation of methane, the second the formation of methanol and the third the formation of hydrogen.

$$\cdot CH_3 + \ \cdot H \xrightarrow{(Ti^{3+}-O)^*} CH_4$$

$$\cdot CH_3 + \ \cdot OH \xrightarrow{(Ti^{3+}-O)^*} CH_3OH$$

$$2 \ \cdot H \xrightarrow{(Ti^{3+}-O)^*} H_2$$

Process flow

0.1 g of the catalyst powder was suspended in 100 ml of 0.2 M NaOH solution. NaOH is the reduction medium. Based on experimental data it is proven that the yields of the products are different depending on which reduction medium is used. At the bottom of the reactor a magnetic stirrer agitated the suspension to prevent sedimentation of the solid catalyst. The temperature, the pressure of the gaseous phase and the pH value of the solution were monitored at all times. After 30 minutes of CO2 bubbling through the suspension to saturate the solution and purge the air out of the reactor the Hg lamp was switched on. The irradiation of the saturated suspension with UV light started the chemical reaction. The CO_2 pressure was constantly held at 110 kPa. At various times during the process samples of the gaseous and the liquid phase were taken by using a syringe and subsequently analyzed. Before the liquid phase could be analyzed the suspension had to be filtered through a Millipore filter membrane to make sure there were no solid particles in the liquid product.

The gaseous product was analyzed in a gas chromatograph, which was equipped with FID and TCD detectors. After a calibration with the calibration gases methane (CH_4), hydrogen (H_2), carbon oxide (CO) and carbon dioxide (CO_2) the gaseous samples were injected. The main product found in the gas phase was CH_4. H_2, oxygen (O_2), nitrogen (N_2) and CO were also detected.

The liquid poduct was analyzed in a gas chromatograph, which was equipped with FID detectors. The main product of the liquid phase was methanol (CH_3OH). Low amounts of ethanol (CH_3CH_2OH) were also detected.

Process flow

Results

The temperature, pressure and the amount of used catalyst during the experimental run is shown in Fig. 2.

CO2	time	pressure	temperature	volume	katalyst
surface	(h)	(Pa)	(°C)	(ml)	(g)
	0				
30647	3,5	121200	33,2	280	0,1
30376	5	120900	34,2	280	0,1
30227	5	117500	33,7	280	0,1
30481	8	116100	34,1	280	0,1
30219	13	117400	34,3	280	0,1
30149	16	113900	35	280	0,1
30228	18	109800	34,7	280	0,1
29632	20	100400	35,4	280	0,1
30070	22	117400	33,2	280	0,1
30138	22	117500	32,8	280	0,1
30028	24	113700	33,4	280	0,1
30665	24	113300	32,6	280	0,1

Fig. 2: Process parameters

Fig. 3 shows the detected products during the process. After five, twenty-two and twenty-four hours control samples were taken to ensure the accuracy of the analysis.

CO2	time	CH4	CH4	CO	CO	H2	H2	H2/100	CH3OH	CH3OH	N2	O2
surface	(h)	(ppm)	(µmol/g kat.)	(ppm)	(µmol/g kat.)	(ppm)	(µmol/g kat.)	(µmol/g kat.)	(µg/l)	(µmol/g kat.)	surface	
	0	0	0	0	0	0	0	0	0	0		
30647	3,5	11,7	1,56	8,4	1,12	0	0,0	0,00		0	473	84
30376	5	27,7	3,67	5,3	0,70	456	60,4	0,60		0	338	61
30227	5	28,5	3,68	6,8	0,88		0,0	0,00		0,00	533	97
30481	8	57,7	7,34	9,3	1,18	535	68,1	0,68	41	1,28	278	41
30219	13	99,8	12,83	12	1,54	834	107,3	1,07		0	319	58
30149	16	114,5	14,25	15	1,87	1040	129,5	1,29	59,1	1,85	340	60
30228	18	130	15,62	16,7	2,01	1207	145,0	1,45		0	358	59
29632	20	144,5	15,84	17,8	1,95	1416	155,2	1,55	58,8	1,84	362	59
30070	22	152,9	19,73	24	3,10	1477	190,6	1,91		0	286	50
30138	22	116	15,00	15	1,94	997	129,0	1,29		0	351	63
30028	24	159	19,86	23,7	2,96	1789	223,5	2,23	72,5	2,27	189	23
30665	24	129,5	16,16	18,7	2,33	1062	132,5	1,33	72,4	2,26	302	49

Fig. 3: Detected products

The main products in the gaseous as well as in the liquid phase are shown in Fig.4, Fig. 5 and Fig.6.

time	CH4	CO	H2/100
hod	(µmol/g kat.)	(µmol/g kat.)	(µmol/g kat.)
0	0	0	0
5	3,67	0,7	0,6
8	7,34	1,18	0,68
13	12,83	1,54	1,07
16	14,25	1,87	1,29
18	15,6	2,01	1,45
20	15,86	1,95	1,55
22	17,35	2,52	1,6
24	18	2,65	1,78

Fig. 4: Products in the gaseous phase

time	CH3OH
hod	(µmol/g kat.)
0	0
8	1,28
16	1,85
24	2,27

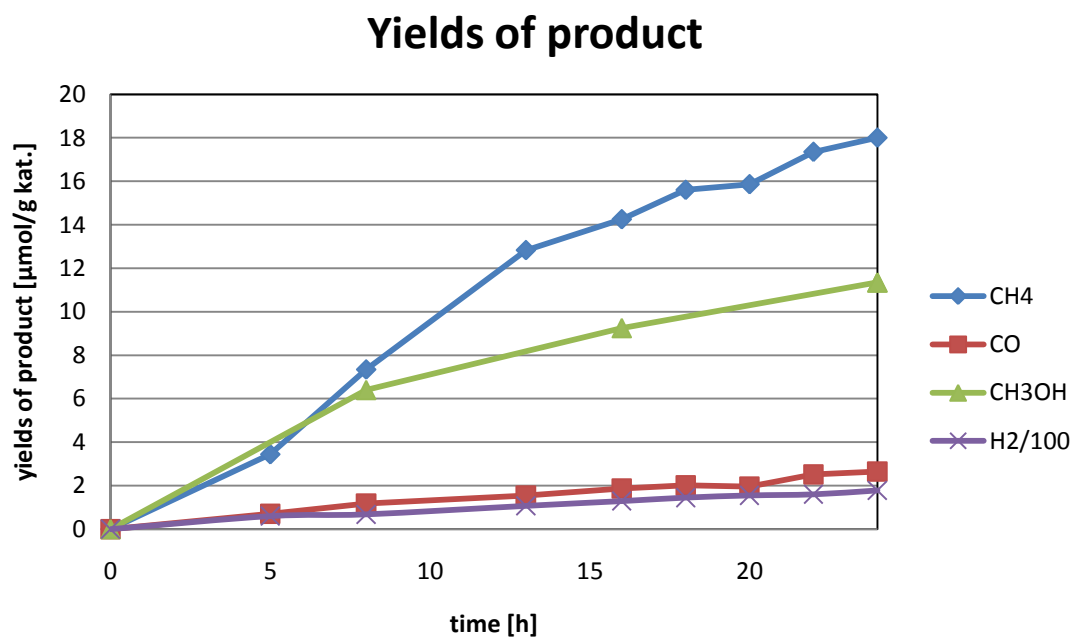Fig. 5: Products in the liquid phase

Yields of product

Fig. 6: Yields of product in the gaseous and the liquid phase

6

References

[1] K. Koči, L. Obalová, L. Matějová, D.Plachá, Z. Lacný, J. Jirkovský, O. Šolcová, Applied Catalysis B:Environmental 89 (2009)

[2] K. Koči, K. Matějů, L. Obalová, S.Krejčíková, Z. Lacný, D.Plachá, L. Čapek, Applied Catalysis B: Environmental 96 (2010)

Catalytic Decomposition of N_2O

Introduction

Nitrous oxide is known to be a very strong greenhouse gas. It has a dramatically high global warming potential and therefore is one of the main contributors of stratospheric ozone destruction. The reduction of nitrous oxide has become an issue of highly importance. Nitrous oxide has been mainly found in flue gases of combustion processes and waste gases of the chemical industry, for example in nitric acid plants. The catalytic decomposition of N_2O offers a simple solution for reducing nitrous oxide. One of the most promising groups of catalysts is calcined layered double hydroxides (LDHs). Layered double hydroxides are layered materials consisting of positively charged hydroxide layers separated by interlayers composed of anions and water molecules. [1]

Experiments

The investigated catalyst in the experiments was Co-Mn-Al mixed oxide with Na. The Co:Mn:Al molar ratio was 4:1:1. It was prepared by impregnation.

The catalytic measurements of the decomposition of N_2O were carried out in fixed bed reactor. The material used for the reactor was stainless steel, since this material does not contribute to the catalyst's performance at the conditions of this experiment. During the measurements the process temperature was between 300°C and 450°C and atmospheric pressure prevails.

The catalytic decomposition of N_2O is shown by the following reaction:

$$2N_2O \rightarrow 2N_2 + O_2$$
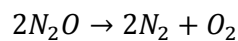
Process Flow

The fixed bed reactor was filled with 0,169 g of the catalyst and was heated by a temperature controlled furnace. Before each experimental run the catalyst inside the reactor was pre-treated by heating a He flow up to 450°C and maintain at this temperature for one hour. Then the catalyst got cooled down to the reaction temperature, which was 400°C for the first and 450°C for the second experimental run, and the feed mixture passed over the catalyst with a volume flow of 56,4 ml/min. After approximately one hour the conversion level of N_2O was constant and considered as the steady state for the calculations. The molar faction of N_2O was measured at the reactor inlet flow as well as at the outlet flow so that the conversion could be calculated. The molar ratio of N_2O was analyzed by a spectrometer.

The molar fractions of N_2O, O_2, and Ar during the whole process are shown in Fig.7. The experimental runs started after 8000 seconds, before that the apparatus was prepared and the calibration was made.
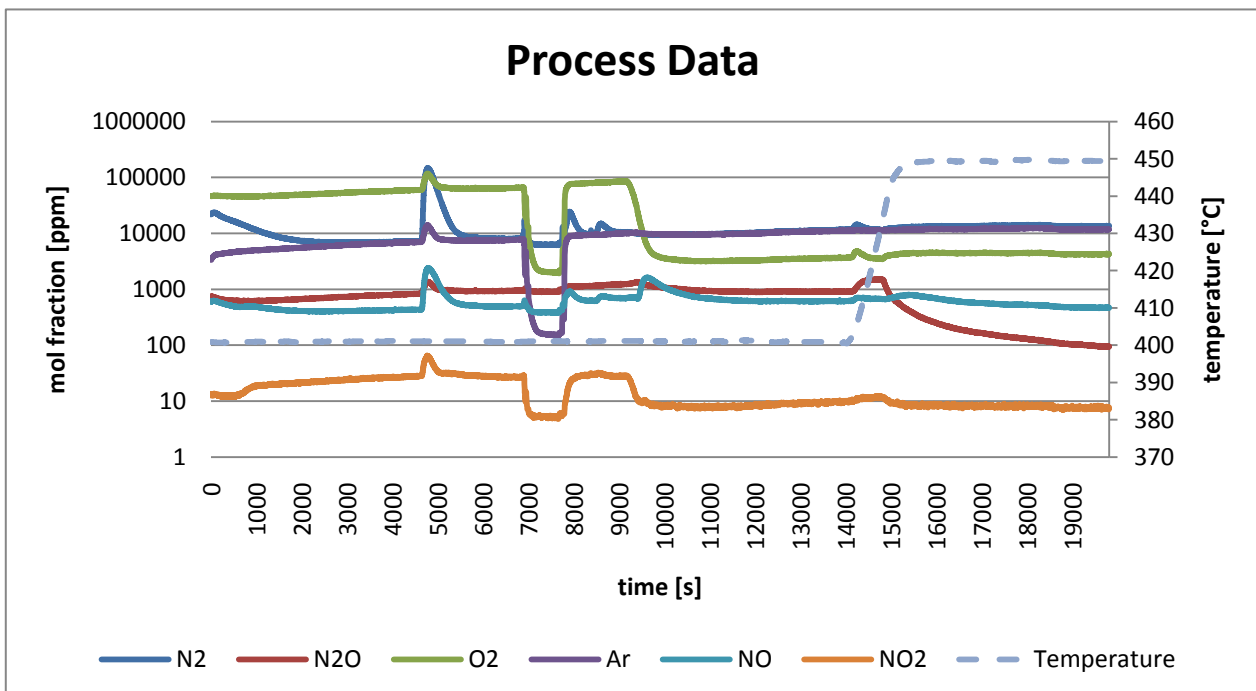

Fig. 7: Process data of the decompostion of NO2

Results

Real gas:	1000 ppm N_2O in He,	Inert gas:	1000 ppm N_2O in He
	5 mol% O_2,		
	3 mol% H_2O,		
	200 ppm NO		

N_2O conversion:

$$X_{N_2O} = \frac{x^0{}_{N_2O} - x_{N_2O}}{x^0{}_{N_2O}} * 100 \qquad [\%]$$

$x^0{}_{N_2O} \dots N_2O \ inlet \ molar \ fraction$

$x_{N_2O} \dots N_2O \ outlet \ molar \ fraction$

N_2O molar fraction:

$$x_{N_2O} = \frac{A_{N_2O}}{f_{N_2O} - A_{Ar}} * x_{Ar} \qquad [mol]$$

$A_{N_2O} \dots. detected \ signal \ of \ N_2O$

$A_{Ar} \dots detected \ signal \ of \ Ar$

$x_{Ar} \dots Ar \ molar \ fraction \ (x_{Ar} = 2000 \ ppm)$

N_2O factor:

$$f_{N_2O} = \frac{1}{f_{Ar}} \qquad [1]$$

Ar factor:

$$f_{Ar} = \frac{Ar}{x_{Ar}} \qquad [1]$$

N_2O conversion for the real gas at 400°C: $X_{N_2O} = 0,592233186 \ \%$

N_2O conversion for the inert gas at 400°C: $X_{N_2O} = 38,20762731 \ \%$

N_2O conversion for the inert gas at 450°C: $X_{N_2O} = 94,02468563 \ \%$

The comparison of those three results is shown in Fig.8. Since the conversion of N_2O at the temperature of 300°C is noticeable low it can most probably be concluded that the used catalyst gets deactivated at these conditions.
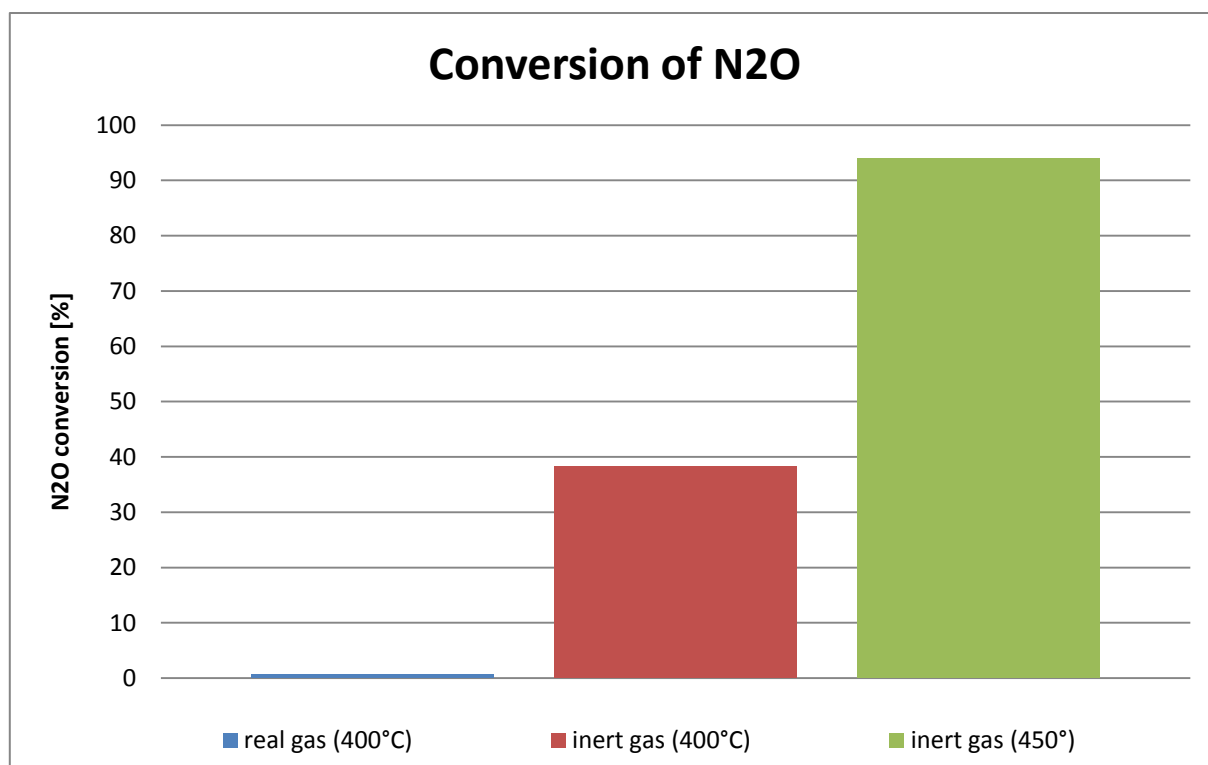
Fig. 8: Conversion of N2O

References

[1] L. Obalová, K. Karásková, K. Jirátová, F. Kovanda, Applied Catalysis B: Environmental 90 (2009)

Adsorption of NO

Introduction

Nitric oxid, is mainly produced by combustion processes, for example in fossil fuel power plants. To decrease the amount of nitric oxides in our stratosphere has become essential. It is necessary to separate the nitric oxide from its carrier gas, which can be achieved by using an adsorption process. Activated carbon has proven to be a very effective adsorbent. [1] The end concentration of nitric oxide can be described by breakthrough curves. There are numerous isotherms, such as the Langmuir or the Freundlich isotherm, describing the sorption behavior of the adsorbent.   [2]

Experiments

The adsorption experiments of NO were held in adsorption column with a diameter of 5cm. Activated carbon was used as adsorbent. Activated carbon is a specific form of carbon which has been processed to make it highly porous and as a result to possess a large surface area available for chemical reactions. The adsorption is mainly caused by the internal surface of the adsorbent thus the influence of the outer surface is negligible.

Process Flow

The flow of the nitric oxide and the carrier gas, nitrogen, were regulated by Aalborg rotameters. The two gases were mixed before they were led into the adsorption column. The outlet was then analyzed by an infra-red analyzer.

Then the breakthrough behavior of the system was described by an adsorption isotherm, the Langmuir isotherm. The Langmuir model, which was first described in 1918, assumes energetically equivalent adsorption centers spread out over the surface of the adsorbent which can only be occupied by one molecule. As a result the model only describes a formation of a monomolecular layer.

Results

Fig. 9 shows the measured data from five experimental runs.

Date	c NO	c NO (20°C)	q	Q	q	c/q
	(mol zl) (-)	g/cm3	ml NO/g	g NO/g	g NO/cm3 au	(-)
19.5.	2,47E-03	3,08E-06	1,61E-01	2,00E-04	1,46E-04	2,11E-02
20.5.	2,14E-03	2,66E-06	2,30E-01	2,87E-04	2,10E-04	1,27E-02
1.6.	2,59E-03	3,23E-06	3,08E-01	3,84E-04	2,80E-04	1,15E-02
6.6.	3,11E-03	3,88E-06	3,03E-01	3,77E-04	2,76E-04	1,41E-02
8.6.	1,80E-03	2,24E-06	2,37E-01	2,95E-04	2,15E-04	1,04E-02

Fig. 9: Measured data may/june

The results from the 19.05.2011 are different than the other measured data and it can be concluded that there was a mistake made during the measurements. For that reason the results from the 19.05.2011 are not used in the following calculations.
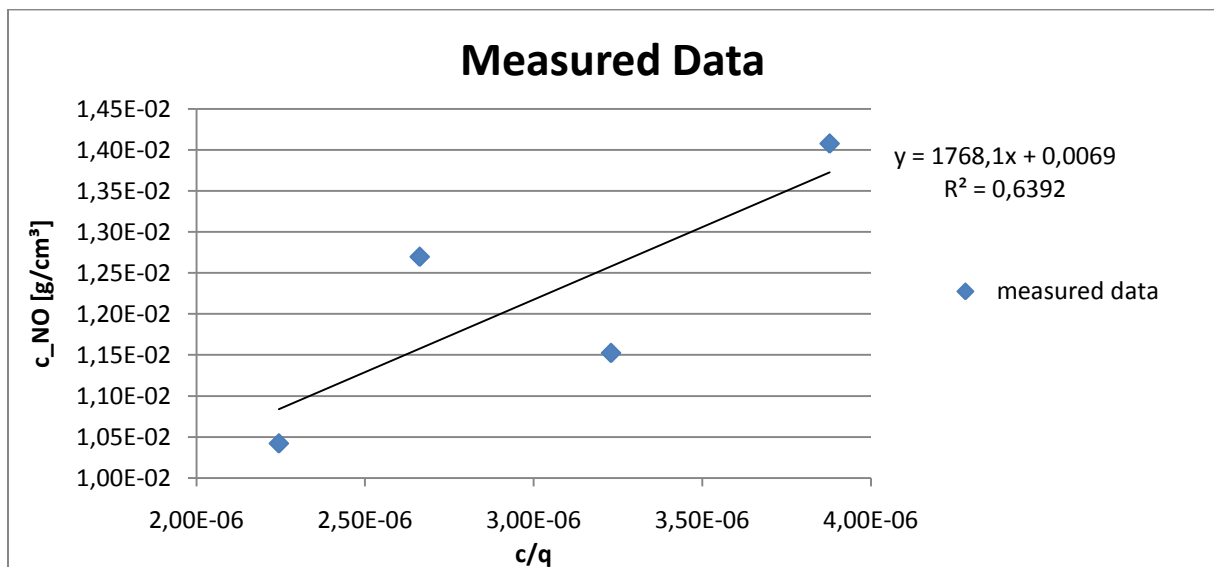

Fig. 10: Measured data and linear equation

The linear equation is shown in Fig.10. Since the measured data don't show a linear trend, the accuracy of the following calculation has to be classified as relatively low.

Langmuir Isotherm:

Linear Langmuir equation:

$$\frac{c}{q} = \frac{1}{q_s} * C + \frac{1}{q_s * K_L}$$

Linear equation of the form $y = k * x + d$

$$y = 1768,1 * x + 0,0069$$

$$k = 1768,1$$

$$d = 0,0069$$

Now q_s and K_L can be found:

$$q_s = \frac{1}{k} = 0,000565579 \text{ [g/cm}^3\text{]}$$

$$K_L = \frac{1}{q_s * d} = 256246,3768 \text{ [cm}^3\text{/g]}$$

Non-linear Langmuir equation: $q = q_s * \frac{K_L * C}{1 + K_L * C}$

Date	q
20.5.	2,29E-04
1.6.	2,56E-04
6.6.	2,82E-04
8.6.	2,07E-04

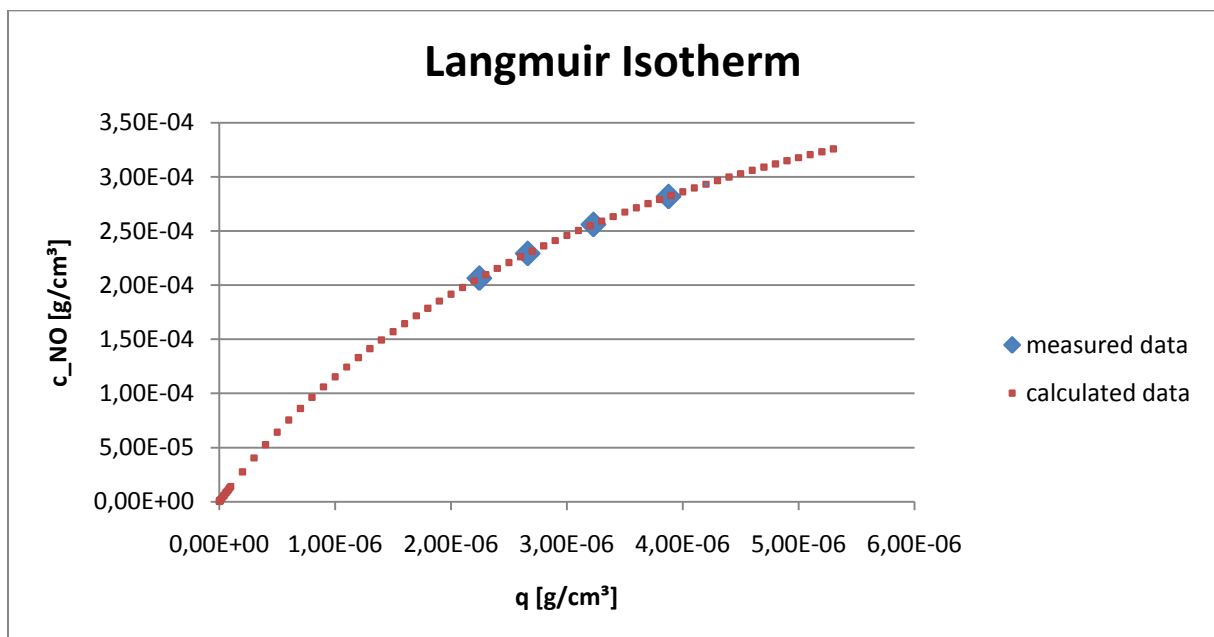Fig. 11: Result of the non-linear Langmuir equation

Fig. 12: Measured and calculated Langmuir Isotherm

14

References

[1] Tirzhá L.P. Datas, Francisco Murilo T. Luna, Ivanildo J. Silva Jr., Diana C.S. de Azevedo, Carlos A. Grande, Alírio E. Rodrigues, Regina F.P.M. Moreira, Chemical Engineering Journal (2010)

[2] Lenka Kubaňová, Lucie Obalová, Oldřich Vlach, Ivana Troppová, Jaroslav Kalousek, Chemical Papers (2011)